To be Submitted for Publication

LBL-8047 C.2
Preprint

EXACT HARD-DISK FREE VOLUMES

W. G. Hoover, N. E. Hoover, and K. Hanson

June 1978

Prepared for the U. S. Department of Energy
under Contract W-7405-ENG-48

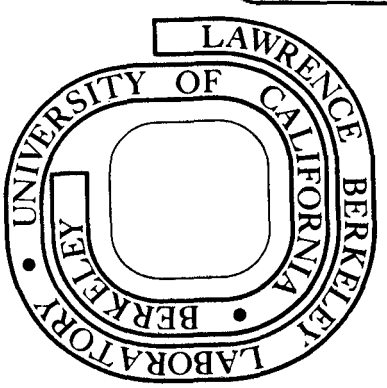

DISCLAIMER

EXACT HARD-DISK FREE VOLUMES

William G. Hoover* and Nathan E. Hoover
Australian National University Computer Centre
Canberra ACT 2600, Australia

and

Kenton Hanson**
Materials and Molecular Research Division
Lawrence Berkeley Laboratory
University of California
Berkeley, California 94720

ABSTRACT:

Properties of exact hard-disk free volumes are determined by a combination of analytical and numerical techniques. Both the high-density solid phase and the lower-density fluid phase are treated. These one particle free volumes are used to verify known thermodynamic information for hard disks and to calculate the shear modulus for the hard disk solid. The free volumes are compared to free volume estimates from the entropy. The statistical distributions of free volume quantities are studied. The percolation transition, at which the free volume changes from extensive (αN) to intensive, is located, and occurs at about one-third of the freezing density.

**Supported by the Division of Materials Sciences, Office of Basic Energy Sciences, U. S. Department of Energy.

I. INTRODUCTION

About forty years ago the concept of free volume was introduced[1,2]. This free volume, the space available to a particle with its neighbors held fixed, was expected to play an important role in understanding fluid motion and structure. The semiquantitative theory of fluids which now exists[3] is not based on these simple ideas but rather on the perturbation description of fluids based upon hard-core system structure. Nevertheless the expectation that the free-volume approach will ultimately prove useful has been responsible for a continuing interest in free volumes.

The development of the Monte Carlo method led to the realization that a cell view of fluid structure is basically correct[4]. Dense-fluid particles are effectively confined to localized regions by their neighbours. In Monte-Carlo simulations it is usual, but not obligatory, to choose moving particles sequentially or at random. One can equally well move each particle many successive times before passing to the next. In such a case the Monte-Carlo chain samples single-particle cells in order to estimate many-particle thermodynamic properties. An alternative view, leading to the same result, pictures a many-particle system containing one particle with small mass. This light particle moves much more rapidly than its more massive slower neighbors, and so appears to sweep out a localized free volume. The relation of one-particle to many-particle theories of fluids was also foreshadowed by some exact relations uncovered in the 1960's[5,6].

In this paper we set out to characterize the free volumes for hard disks in a quantitative way. The two-dimensional problem can be analyzed more completely than the three-dimensional one, although we have recently obtained new three-dimensional results as well[7]. The four goals motivating this work are summarized below:

I. Relation of thermodynamic information to the free volumes. Although the relations to the pressure and chemical potential are well known, the approximate relationship between free volume and entropy and the exact relationship between free volume and the elastic constants had not been investigated.

II. Investigation of nucleation and cluster theory for a tractable but nontrivial continuum model.

III. Location of the percolation transition marking the change of free volume from extensive (αN) to intensive as the number density increases.

IV. Investigation of the usefulness of high-level programming languages, such as Simula 67, to logically complex tasks such as the determination of the free volumes. This goal was eventually abandoned as the imagined advantages of Simula 67 vanished on closer inspection.

II. FREE VOLUMES

Two different kinds of free volumes have been defined and used for hard particles. One is the space v_f' available to a new particle. This extensive quantity gives a direct measure of the constant volume chemical potential relative to an ideal gas[5,6,8]:

$$\mu^e/kT = \ln(V/v_f') \tag{1}$$

Adams[8] has recently verified the usefulness of (1) for densities up to half the close-packed hard-sphere density.

If we ask, on the other hand, how much space is available to an existing particle, the answer v_f is extensive only at low density (when

both kinds of free volume are identical and given by (1). At higher densities the existing-particle free volume is localized and intensive.

The free volume v_f for existing particles is simply related to the pressure :

$$PV/NkT = 1 + (\sigma/2D)\langle s_f/v_f \rangle \qquad (2)$$

where s_f is the surface of the free volume (perimeter in two dimensions) and D is the number of dimensions (2 for disks). Pressure is usually determined from the virial theorem or the collision rate in computer experiments. These estimates agree well with the theoretically-based estimates based on the virial series[9,10,11,12,13].

To estimate the pressure from (2) the ratio of surface to free volume is calculated for each particle in the system and these quotients are then averaged.

Approximate thermodynamic properties are often calculated from a cell model in which one particle moves in the potential due to its fixed neighbors[14]. This cell-model approximation leads also to an equation like (2) above, but with $2D$ replaced by D. Thus the true free volumes are not only less regular in shape, but also smaller than those of the cell model. Cell-model approximations to the free energy[15] and heuristic predictions of the melting transition[16] have both proved to be surprisingly good.

Systematic cell-cluster attempts to improve the simple cell picture[17,18] appear to converge slowly, particularly in two dimensions. More sophisticated approaches have provided excellent free energy estimates for solid-phase disks and spheres[19].

By following the scheme outlined in appendix A we have measured exact

free volumes in a series of 48 disk and 192 disk systems. In these calculations all N particles are allowed to move, and the volumes available to each are computed after every 10N accepted moves. Figure 1 illustrates the free volumes for the three qualitatively different cases:

(I) .Low-density fluid with extensive v_f and s_f.

(II) .Dense fluid with intensive v_f and s_f.

(III) .Solid with intensive v_f and s_f.

Our 48 disk results establish (as we had expected[4]) that fluid free volumes are smaller than solid free volumes at the same density. Near the freezing density there is an increase of about 20% in $\langle v_f \rangle$ on going from the fluid to the solid phase. This difference is caused by the relative packing inefficiency of the disordered irregular fluid structure.

The results are summarized in Table I. Data for densities of 0.20, 0.25, and 0.30 are relatively unreliable. This is because the region associated with the percolation transition, discussed below, involves treating periodic free volumes which span the system horizontally, or vertically, or diagonally. The many special cases which arise in this region cannot all be handled by the methods outlined in the appendix, and so our results are based on a few configurations generated before such an exceptional case arose. Table I relates the mean values from these computer experiments to the known (Padé Approximant) results for pressure, chemical potential, and entropy. In Figure 2 we illustrate the remarkably simple dependence of the dense-fluid free volumes on density. Both $\langle \ln v_f \rangle$ and $\ln \langle v_f \rangle$ vary almost linearly with density. Approximate cell theories and simple assumed relations between entropy or free energy and $\ln v_f$ predict a more complicated density dependence.

At each density the fluctuations in v_f and s_f can be used to determine the exponent a in the probability densities,

$$p(x) \propto x^a \exp(-bx) \tag{3A}$$

for the free volume, and

$$p(x) \propto x^a \exp(-bx^2) \tag{3B}$$

for the free surface. These forms are suggested by Meijering's work on the distribution of Voronoi polyhedra volumes and surfaces[20]. Kiang[21] was able to verify such a relation numerically, in both two and three dimensions, for random distributions of points.

Our results suggest that the exponent a in the free volume distribution is approximately 0.1 for the dense fluid and approximately 0.6 for the free surface distribution. We do not tabulate the fluctuations as functions of density because the precision of the data does not warrant it. The data suggest that a increases slightly with density, but more extensive calculations on larger systems would be required to establish this. If the free volume distribution at fixed density were exponential (a=0) then $\ln\langle v_f\rangle - \langle \ln v_f\rangle$ would be Euler's constant, 0.577. The slightly smaller offset, 0.4 or so, corresponds to the small nonzero value of a.

III. ELASTIC CONSTANTS

The standard expressions for the elastic constants are derived from the partition function by differentiating twice with respect to the thermodynamic strains[22]. The resulting ensemble averages involve the second derivative of the interparticle pair potential and the square of the first derivative. Because both these averages diverge for hard particles, an alternative route to the elastic constants is desirable. We characterize

them through the free volume. It is possible to show that the collisional parts of the pressure tensor components correspond to averaged momentum transfers along the perimeter of the free volume. The shear stress $-P_{xy}$, for example, can be calculated by carrying out integrals of $\sin\theta\cos\theta$ around the free-volume perimeter:

$$P_{xy}V/NkT = \tfrac{1}{2}\sigma^2 < \sum \int \sin\theta_i \cos\theta_i d\theta_i / v_f > . \qquad (4)$$

θ_i is measured counterclockwise relative to the x axis. The θ integrations in (4) are carried out in a series of coordinate systems centred on the (three to six) disks contributing the central particle's free-volume boundaries. The periodic crystal is maintained at constant macroscopic shear strain during the calculation.

For two-dimensional crystals with hexagonal symmetry the linear shear modulus is independent of orientation. For very large strains this symmetry is lost. Direct evaluation of the shear modulus, using Eq. (4), for relatively small strains gives the shear-modulus estimates listed in Table II. Although the strains actually used might exceed the elastic limit for an infinite crystal, unsmoothed cell-model calculations suggest that the finite-strain results at these strains should lie within about a percent of the zero-strain limit in which the moduli are defined. At strains somewhat smaller than those we have chosen, the pressure fluctuations become so severe that even the sign of P_{xy} becomes uncertain. Our results have uncertainties of several percent due to the relatively large fluctuations in the hard-disk free volumes.

There are several ways to estimate the shear modulus theoretically. The cell model approximation to the Helmholtz free energy can be used to derive (4) without the 2 which appears in the denominator. By evaluating this expression we find that the cell-model shear modulus is much too

large (see Table II). In three dimensions even larger disparities between cell-model and thermal shear moduli have been found using the Lennard-Jones and exponential-six potentials[22].

Despite the fact that the three-particle cell-cluster correction is much larger than the already large two-particle correction, the final cell-cluster prediction for the shear modulus is in error by only 30%. This theory predicts an infinitesimal-strain high-density shear modulus equal to 0.494 times the cell-model prediction. Because the theoretical finite-strain and finite-density corrections are unknown, we have used the same correction factor, 0.494, in the Table II cell-cluster estimates. An extension of Barker and Gladney's work[19] might well provide sound theoretical estimates for hard-disk and hard-sphere shear moduli.

For crystals in which the interactions are purely harmonic between nearest neighbors the shear modulus is equal to half the bulk modulus. Unfortunately the isothermal and isentropic bulk moduli differ by roughly a factor of three for hard disks (Table II). The results we find lie closer to the isothermal estimate.

In two dimensions the maximum value of Poisson's Ratio ($\lambda/[\lambda+2\eta]$ in terms of the Lamé Constants) is one, the value for an incompressible material, while harmonic forces give one third. For hard disks the relatively great heating associated with isentropic compression gives a much larger Poisson's Ratio than that found for isothermal compression.

IV. NUCLEATION AND CLUSTER THEORY

In computing the free volume at low density it is possible to consider the system as being composed of clusters, a cluster consisting of contiguous particles lying within 2σ of their neighbors. At low enough density one can calculate the partition functions for clusters of 1, 2, 3, ... particles, and using the grand partition function, calculate the number of clusters as a function of density. Recent calculations for overlapping disks carry the expansion through terms of fourth order in the density[23]. For nonoverlapping disks the calculation is more difficult, and we have not pursued it beyond the simple two-particle terms given below.

We have calculated the first three partition functions, for clusters of 1 and 2 particles. We have (using Hill's notation)[24]:

$$\begin{aligned} Y_{100} &= V \\ Y_{200} &= V[V-1.5B] \\ Y_{010} &= V[1.5B] \end{aligned} \qquad (5)$$

For disks with second virial coefficient $B = 1.8138V_o$, the 1.5 becomes 2.0 if the disks are allowed to interpenetrate. The simple cluster partition functions can then be used[24] to compute the densities of physical clusters of various sizes. The percolation transition[25,26,27] is signalled by the divergence of the average cluster size[27].

The average cluster size diverges at a percolation density, relative to close-packing, of about 0.245 ± 0.02. The estimate in reference 23, for overlapping disks corresponds, in our units, to 0.32, plus or minus 6%.

Figure 3 shows the variation in the average cluster size with density. The data indicate a transition at a density (relative to close-packing) of 0.245. At this density the thermodynamic-limit probability for finding a

particle in the largest cluster rises abruptly from zero. The "percolation" density found here agrees with a short extrapolation of the data of Pike and Seager[28]. Those authors use a method for generating configurations which is different from that used for hard disks, but the difference is unimportant at the low densities they considered.

The rise of cluster size is thought to vary with $\delta\rho$ as (about) the inverse 19/8 power[23,27,29]. An approximate model (predicting 20/8) can be based on the idea that clusters of size j have a total surface area which is independent of j-- This condition incorporates the picture that clusters grow and decay through surface collisions. If the surface area of an individual cluster varied as $j^{\frac{1}{2}}$, then the number of j clusters would vary as

$$N(\rho/\rho_c)^j/j^{\frac{1}{2}}. \tag{6}$$

Integration of j^2 over this distribution gives the average cluster size (each j cluster contains j particles with cluster size j):

$$S \propto N(\rho/\rho_c)^{-5/2} \propto N/\delta\rho^{5/2} \tag{7}$$

where $\delta\rho$ is the density difference relative to the percolation density.

Fisher[26] outlines a slightly different approximate model which is closer to numerical estimates in three dimensions[23] but less close in two.

V. REMARKS

The data given here characterize quantitatively the available one-particle states in a hard-disk system. The free-volume distribution at each density is approximately exponential, as is also the dependence of the average free volume on density. These two results should serve as useful guides in constructing and improving cell theories of the fluid state[30]. Neither of these simple relations has so far been predicted theoretically.

APPENDIX A

The free volumes are calculated by first locating, for each configuration to be analyzed, the "nodes" formed by the intersections of pairs of "exclusion disks" of radius σ. Ordered (by angle) pairs of these nodes are then connected together to make "circuits" and the areas and perimeters of these circuits are expressed as polar-coordinate integrals. The periodic boundary conditions complicate the task but reduce the number-dependence sufficiently to make their use essential. Higher-level computing languages which use recursion and dynamic storage allocation, such as Simula 67, might seem better suited to this task than Fortran. At the same time the relative inefficiencies in writing and compiling the high-level languages must be considered. The flow chart below is a summary of the method used in our free volume calculations.

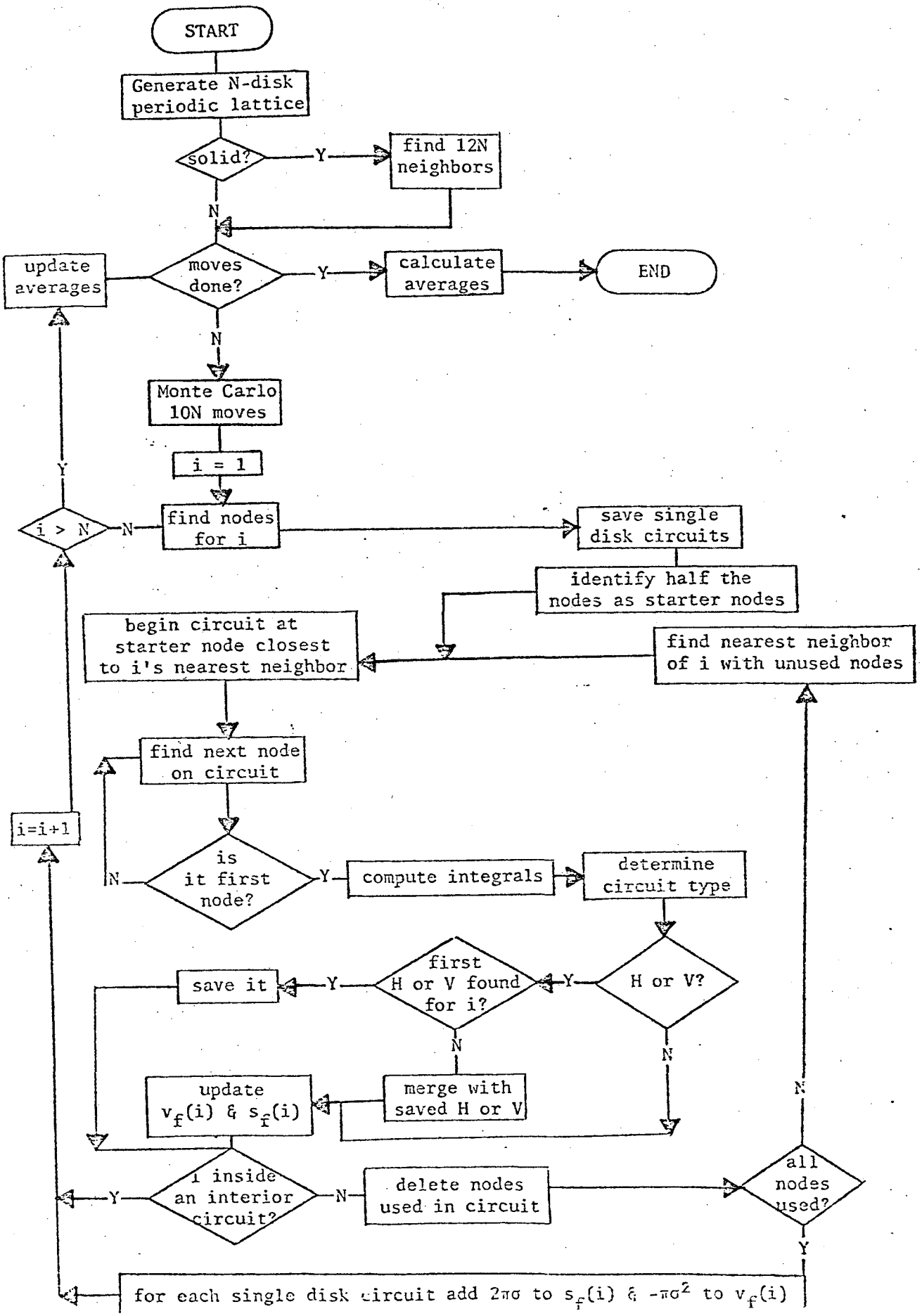
START
Generate N-disk periodic lattice
solid?
Y
find 12N neighbors
N
update averages
moves done?
Y
calculate averages
END
N
Monte Carlo 10N moves
i = 1
Y
i > N
N
find nodes for i
save single disk circuits
identify half the nodes as starter nodes
begin circuit at starter node closest to i's nearest neighbor
find nearest neighbor of i with unused nodes
find next node on circuit
i=i+1
N
is it first node?
Y
compute integrals
determine circuit type
save it
Y
first H or V found for i?
Y
H or V?
N
N
update $v_f(i)$ & $s_f(i)$
merge with saved H or V
i inside an interior circuit?
Y
N
delete nodes used in circuit
all nodes used?
N
Y
for each single disk circuit add $2\pi\sigma$ to $s_f(i)$ & $-\pi\sigma^2$ to $v_f(i)$

REFERENCES

*Fulbright-Hayes Fellow, 1977-1978. This work was partially supported by the Fulbright-Hayes Foundation, by the Lawrence Livermore Laboratory (permanent address) and by the University of California at Davis-Livermore. M.R. Osborne and R.O.W. Watts of the ANU Computer Centre generously provided office space and 100 hours of computer time on the Univac 1100/42.

1. H. Eyring & J.O. Hirschfelder, J. Phys. Chem. 41, 249 (1937).
2. J.E. Lennard-Jones & A.F. Devonshire, Proc. Roy. Soc. (London), A163 53 (1937); A165, 1 (1938); A169, 317 (1939); A170, 464 (1939).
3. J.A. Barker & D. Henderson, Revs. Mod. Phys. 48, 587 (1976).
4. W.G. Hoover, W.T. Ashurst, & R. Grover, J. Chem. Phys. 57, 1259 (1972).
5. W.G. Hoover and J.C. Poirier, J. Chem. Phys. 37, 1041 (1962).
6. B. Widom, J. Chem. Phys. 39, 2808 (1963).
7. K. Hanson & W.G. Hoover, Work in progress.
8. D.J. Adams, Mol. Phys. 28, 1241 (1974).
9. W.G. Hoover & B.J. Alder, J. Chem. Phys. 45, 2361 (1966).
10. W.G. Hoover & F.H. Ree, J. Chem. Phys. 49, 3609 (1968).
11. B.J. Alder, W.G. Hoover, & D.A. Young, J. Chem. Phys. 49, 3688 (1968).
12. W.G. Hoover & B.J. Alder, J. Chem. Phys. 46, 686 (1967).
13. K.W. Kratky, Physica 85A, 607 (1976).
14. R.J. Buehler, R.H. Wentorf, J.O. Hirschfelder, & C.F. Curtiss, J. Chem. Phys. 19, 61 (1951).
15. L.V. Woodcock and K. Singer, Trans. Farad. Soc. 67, 12 (1971).
16. B.J. Alder, W.G. Hoover, & T.E. Wainwright, Phys. Rev. Lets. 11, 241 (1963).
17. F.H. Stillinger and Z.W. Salsburg, J. Chem. Phys. 46, 3962 (1967).
18. F.H. Stillinger, Z.W. Salsburg, & R.L. Kornegay. J. Chem. Phys. 43, 932 (1965).

19. J.A. Barker & H.M. Gladney, J. Chem. Phys. 63, 3870 (1975).

20. J.L. Meijering, Philips Res. Rep. 8, 270 (1953).

21. T. Kiang, Z. Astrophys. 64, 433 (1966).

22. A.C. Holt, W.G. Hoover, S.G. Gray, & D.R. Shortle, Physica 49, 61 (1970).

23. S.W. Haan & R. Zwanzig, J. Phys. A 10, 1547 (1977).

24. T.L. Hill, J. Chem. Phys. 23, 617 (1955).

25. S.R. Broadbent & J.M. Hammersley, Proc. Camb. Phil. Soc. 53, 629, 642 (1957).

26. M.E. Fisher, Rept. Prog. Phys. 30, 615 (1967).

27. J.W. Essam, Phase Transitions & Critical Phenomena, Vol 2, Ch 6, (C. Domb & M.S. Green, Eds) Academic, London (1972).

28. G.E. Pike & C.H. Seager, Phys. Rev. 10B, 1421 & 1435 (1974).

29. I. Enting and W.T. Ashurst (Stimulating conversations).

30. D.J. Adams and A.J. Matheson, J. Chem. Soc., Faraday II, 68, 1536 (1972) and Chem. Phys. Letters 22, 484 (1973).

FIGURE CAPTIONS

1. Configurations of hard disks at densities of $\rho = 0.20$, 0.50, and 0.80 relative to close packing. At the two lower two densities "exclusion disks" are drawn around each particle. These indicate the areas from which neighboring particles are excluded. At $\rho = 0.20$ the particles form seven clusters and all 48 free volumes are extensive. At $\rho = 0.80$, in both the fluid and solid phases, the free volumes are drawn for each particle. These free volumes are small and intensive.

2. Variation of 48-disk free volume v_f and entropy with density. S^e is the entropy relative to that of an ideal gas at the same density. $(S^e/Nk) + 0.856$ is plotted for comparison with the measured free volumes. The data can be described within about 0.10 by the straight-line relation $\ln(\langle v_f \rangle/d^2) = 3.9 - 9.6\rho$, where ρ is 1.00 at close-packing. Note also that $\ln(v_f/d^2) = \ln(Nv_f/V) - 0.144$. Also shown is the approximation to $\ln(v_f/d^2)$ calculated from the unsmoothed cell model. The cell model predicts a transition density, from extensive to intensive free volumes, at $\rho = 0.25$. (d is the nearest-neighbor spacing in the perfect triangular lattice.)

3. Variation of average cluster size with density. The low-density linear decrease can be calculated from theory[24]. In the solid the number of single-particle clusters can be estimated by cavity-formation calculations. It is at most $N/10^{12}$. In the Figure we show the inverse cluster size from Monte Carlo calculations (50 configurations at each density). These data have been adjusted by increasing the offset from the low-density limit, $1 - (1/S)$, by $N/(N-1)$. The fit shown in the Figure is given by $1/S = 28.8(\rho - 0.245)^{2.4}$.

TABLE I. Comparison of thermodynamic data for hard disks with properties of the computer-generated free volumes. Except as indicated, these results are for 50 48-disk configurations or 25 192-disk configurations. The angular brackets indicate Monte-Carlo values. The volume per particle is $\sqrt{3/4}$ and $\sigma = \rho^{\frac{1}{2}}$ is the hard disk diameter. $(Z-1)4/\sigma$ is the estimated value of $\langle s_f/v_f \rangle$ for an infinite system. Our results are a few percent lower, primarily due to finite-system center-of-mass motion[12]. At low density $\mu^e/kT + \ln\langle v_f \rangle$ approaches $\ln(v)$, 3.73 for 48 disks. For the solid-phase infinite-system estimates we have used $(S-S_{cell})/Nk = 0.05$ in the high-density limit[10,11].

V_o is the close-packed volume, $\sqrt{3}\,\sigma^2/2$. The triangular-lattice interparticle spacing is chosen as the unit of length. The Monte-Carlo jump length used was $\sigma((V/V_o)^{\frac{1}{2}} - 1)$.

TABLE 1

N	V_o/V	$\langle s_f \rangle$	$\langle v_f \rangle$	$\langle s_f/v_f \rangle$	$(Z-1)4/\sigma$	$\ln\langle v_f \rangle$	μ^e/kT	$\langle \ln v_f \rangle$	S^e/Nk
48	0.050	58.88	34.47	1.71	1.74	3.54	0.19	3.54	-0.09
48	0.100	73.29	27.91	2.63	2.67	3.33	0.41	3.33	-0.20
48	0.150	76.96	21.93	3.52	3.54	3.09	0.65	3.09	-0.31
*48(12)	0.200	71	16.7	4.41	4.46	2.81	0.92	2.79	-0.42
*48(1)	0.250	64	11	6	5.47	2.4	1.24	2.3	-0.56
*48(4)	0.300	18	3.7	6.5	6.61	1.22	1.60	0.88	-0.70
48	0.350	11.90	1.92	7.65	7.93	0.65	2.03	0.28	-0.86
48	0.400	6.97	1.00	9.25	9.49	-0.00	2.54	-0.38	-1.03
48	0.450	4.56	0.59	11.00	11.38	-0.53	3.14	-0.91	-1.23
48	0.500	3.31	0.37	13.26	13.71	-1.00	3.88	-1.38	-1.46
48	0.550	2.46	0.24	16.19	16.63	-1.43	4.80	-1.85	-1.72
48	0.600	1.858	0.155	19.64	20.38	-1.86	5.97	-2.30	-2.02
48	0.625	1.650	0.126	22.2	22.68	-2.07	6.68	-2.54	-2.20
48	0.650	1.417	0.0979	25.3	25.34	-2.32	7.49	-2.82	-2.38
48	0.675	1.249	0.0776	27.4	28.43	-2.56	8.43	-3.02	-2.59
48	0.700	1.067	0.0579	32.5	32.07	-2.85	9.53	-3.33	-2.82
48	0.725	0.943	0.0476	35.3	36.39	-3.05	10.82	-3.53	-3.07
48	0.750	0.849	0.0389	35.8	41.56	-3.25	12.35	-3.65	-3.35
48	0.775	0.727	0.0291	43.6	47.84	-3.54	14.20	-4.00	-3.67
48	0.800	0.624	0.0218	48.9	55.57	-3.83	16.46	-4.27	-4.04
+48	0.800	0.680	0.0261	39.4	40.77	-3.64	13.06	-3.96	-3.95
+48	0.850	0.498	0.0144	52.1	53.69	-4.24	16.96	-4.53	-4.59
+48	0.900	0.321	0.0061	76.7	80.04	-5.10	24.44	-5.38	-5.46
+48	0.950	0.158	0.0015	154.9	159.80	-6.50	45.83	-6.79	-6.89
+192	0.900	0.319	0.0061	79.4	80.04	-5.11	24.44	-5.42	-5.46

* The uncertainty in v_f is typically 1-2%. Entries marked with an asterisk(*) are based on fewer configurations and are less accurate.

\+ These are single-occupancy solid-phase runs.

TABLE II. Shear modulus for hard disks from free volumes. In these calculations each particle is confined to a circular cell of diameter equal to the perfect-crystal triangular lattice spacing d. The shear modulus estimates from the finite-strain cell model and the high-density cell cluster theory are included. The last two columns give half the isothermal and adiabatic bulk moduli for disks. These shear modulus estimates would be appropriate for a harmonic crystal. The uncertainties in P_{xy} and η are about 20%.

N	V_o/V	ϵ_{xy}	$P_{xy}V/NkT$	$\eta V/NkT$	Cell	Cell-Cluster	Harmonic
48	0.850	0.020	-0.77	38	71	35	44 or 133
192	0.850	0.020	-1.03	52	71	35	44 or 133
48	0.900	0.010	-1.22	122	174	86	100 or 299
192	0.900	0.010	-1.37	137	174	86	100 or 299
48	0.950	0.005	-2.98	596	752	371	400 or 1197
192	0.950	0.005	-2.07	413	752	371	400 or 1197

ρ=0.200 FLUID

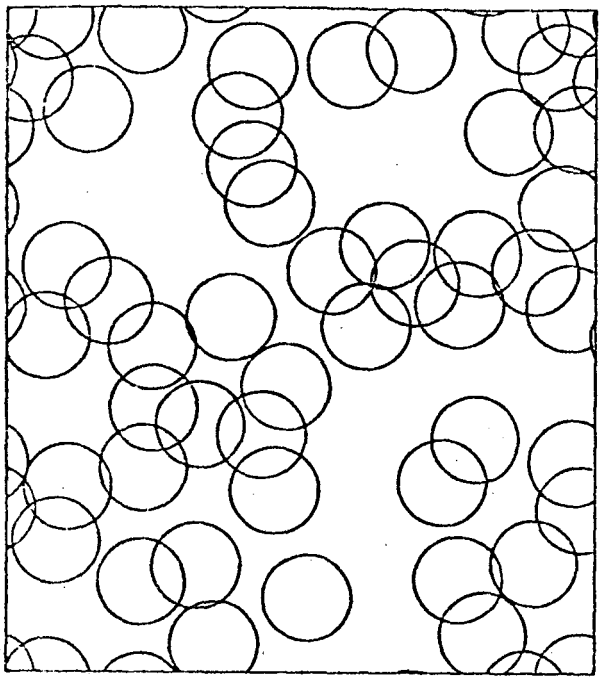

ρ=0.500 FLUID

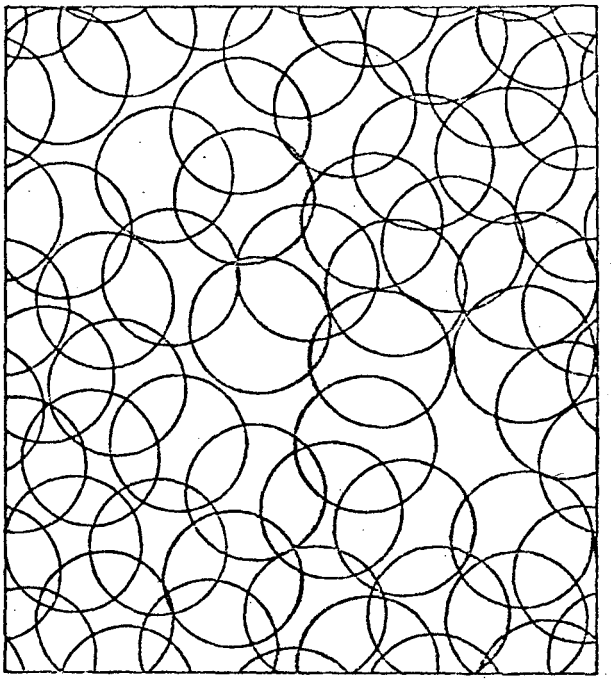

ρ=0.800 FLUID

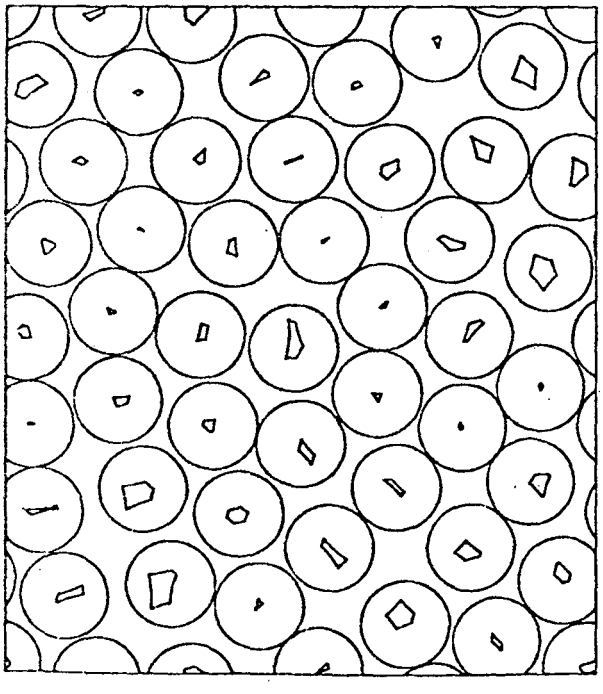

ρ=0.800 SOLID

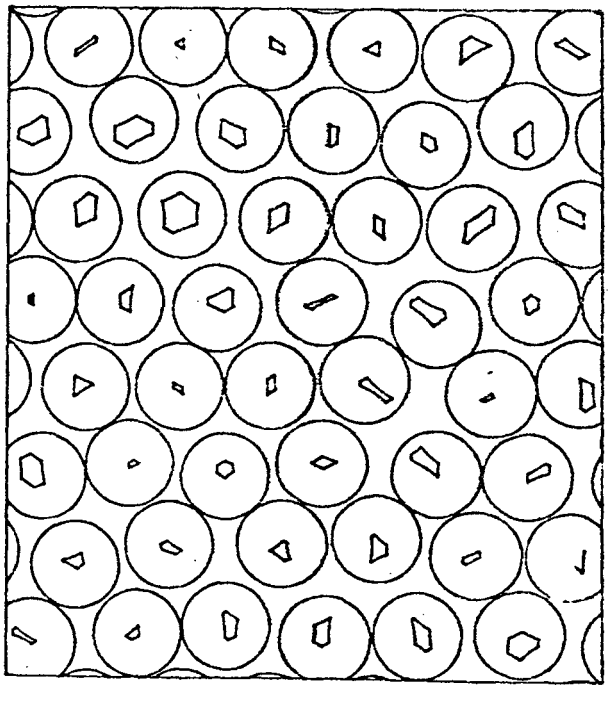

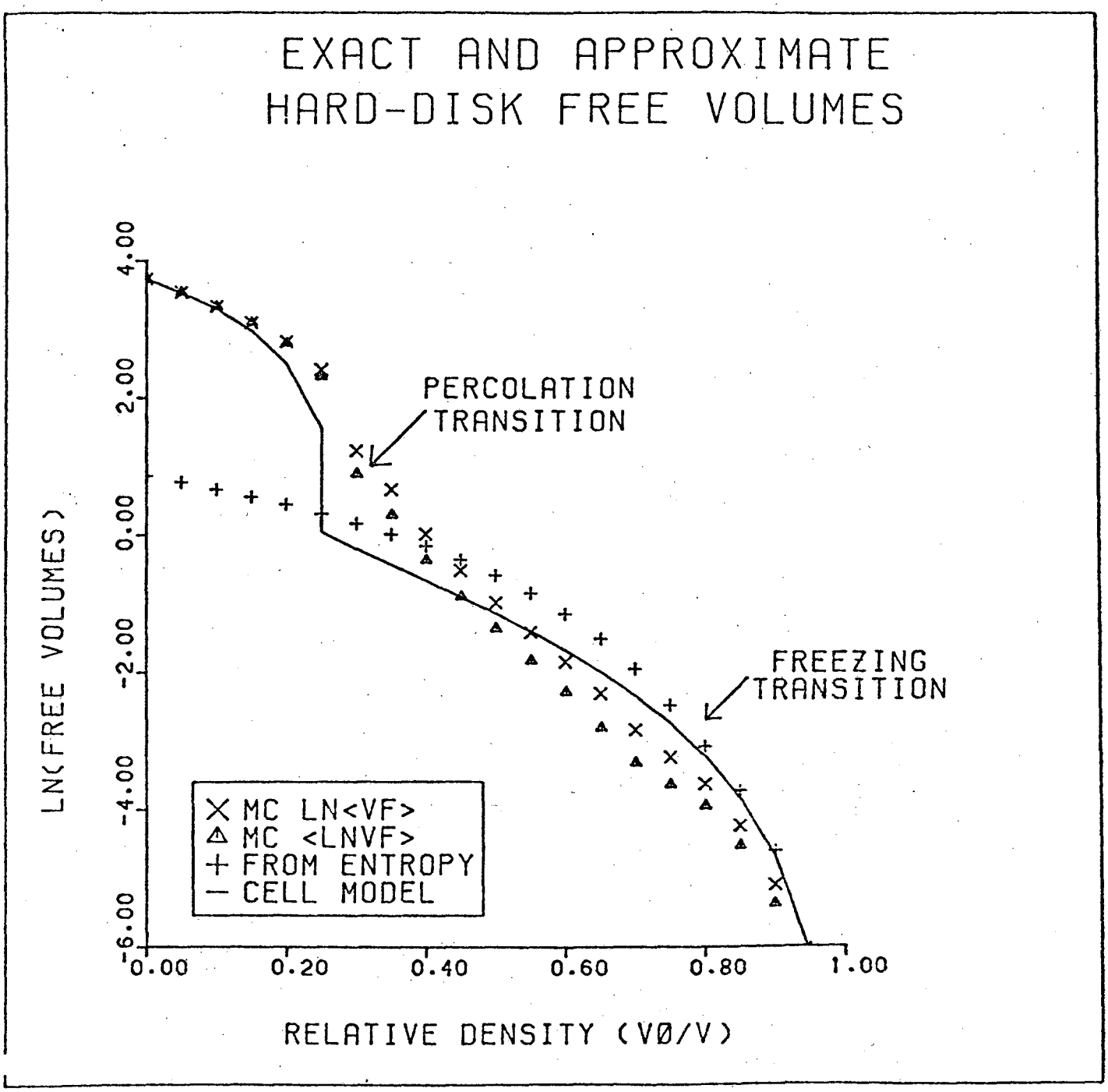
EXACT AND APPROXIMATE
HARD-DISK FREE VOLUMES
LN(FREE VOLUMES)
4.00
2.00
0.00
-2.00
-4.00
-6.00
0.00
0.20
0.40
0.60
0.80
1.00
RELATIVE DENSITY (VØ/V)
PERCOLATION
TRANSITION
FREEZING
TRANSITION
MC LN<VF>
MC <LNVF>
FROM ENTROPY
CELL MODEL

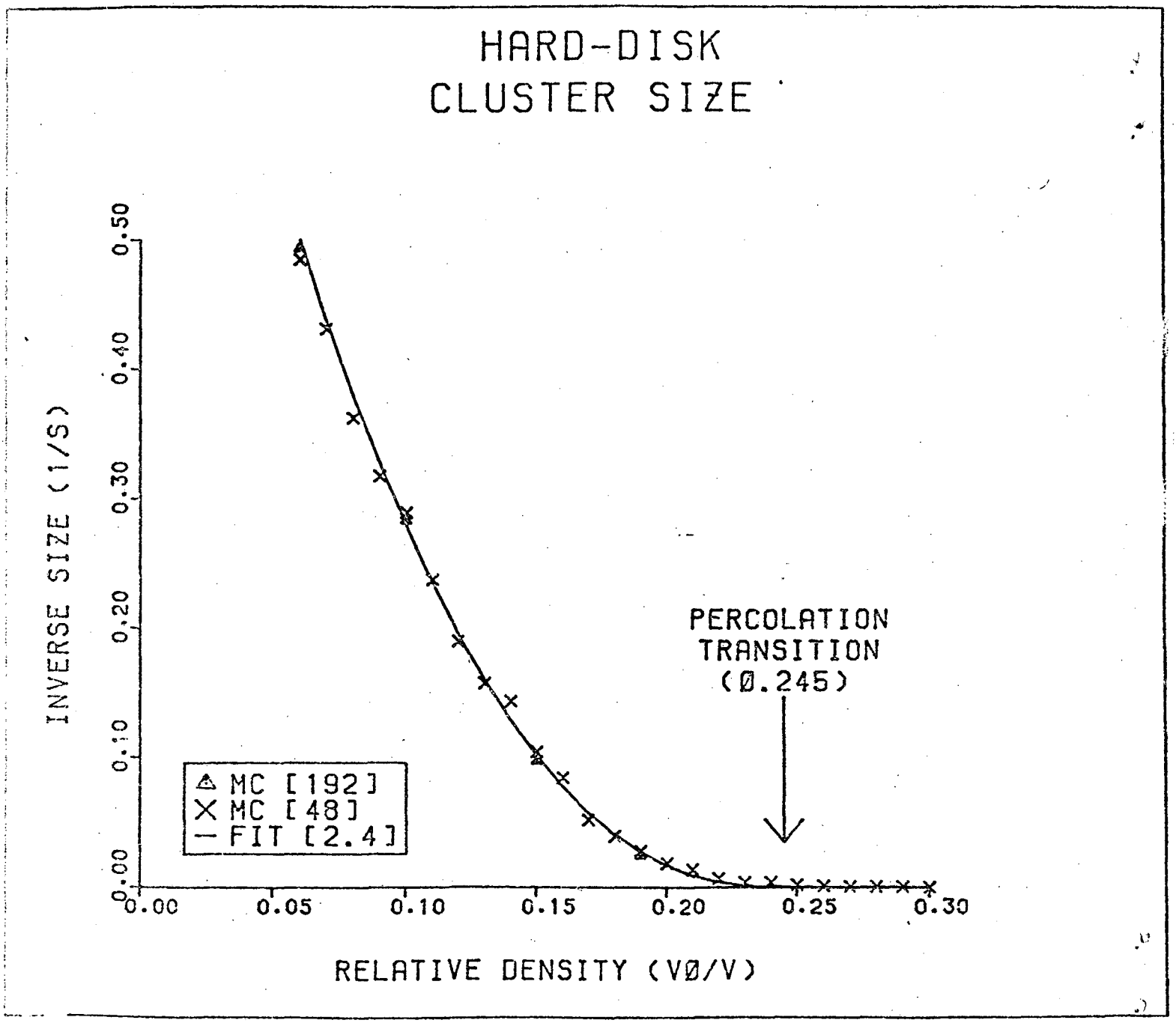
HARD-DISK
CLUSTER SIZE
INVERSE SIZE (1/S)
0.00
0.10
0.20
0.30
0.40
0.50
0.00
0.05
0.10
0.15
0.20
0.25
0.30
RELATIVE DENSITY (VØ/V)
PERCOLATION
TRANSITION
(Ø.245)
MC [192]
MC [48]
FIT [2.4]

TECHNICAL INFORMATION DEPARTMENT
LAWRENCE BERKELEY LABORATORY
UNIVERSITY OF CALIFORNIA
BERKELEY, CALIFORNIA 94720